A Study of the Seismic Response of Asphaltic Concrete Used as a Core in Rockfill Dams

Ali Akhtarpour[1*] and Ali Khodaii[2]

1. Assistant Professor, Ferdowsi University of Mashhad, Mashhad, Iran,
* Corresponding Author; email: akhtarpour@um.ac.ir
2. Associate Professor, Amirkabir University of Technology, Tehran, Iran

Received: 21/02/2015
Accepted: 16/12/2015

ABSTRACT

Seismic response of the asphaltic concrete used as an impermeable core of a rockfill dam was investigated. In the first part of the study, geotechnical parameters of the asphaltic concrete were obtained from a series of monotonic and cyclic triaxial tests. In the second part, 2D and 3D Nonlinear numerical analyses were performed for the highest dam with asphalt concrete core in Iran (Shur River Dam) under seismic forces. Different stages of construction and reservoir filing were analysed using the hyperbolic model with finite difference method. Both 2D and 3D analysis confirms that the earthquake shock can lead to developing some cracks and increasing permeability of asphalt in the upper part of the core; moreover, maximum vertical deformations occur near the crest and at the lower part of the upstream slope. The pattern of the core deformation in 2D analysis includes settlements of the shells behind the asphaltic core and the core remains upright, but 3D analysis shows that the core can settle with the neighbouring shells. Furthermore, 2D analysis shows more settlements in the shells and less crest accelerations in comparison with 3D analysis. Shear strains in the asphaltic core have different trends in the two types of analyses.

Keywords:
Dynamic behaviour; Nonlinear dynamic analysis, Asphaltic concrete core dam, Newark approach, Equivalent linear analysis

1. Introduction

Asphaltic concrete (AC) has been used for 50 years as an impervious interior core walls in hydraulic structures such as embankment dams. Significantly important engineering properties of the asphaltic concrete used in hydraulic structures are: workability during pouring and compaction, impermeability, flexibility and ductility to avoid cracking as a result of unfavourable field stress and deformation conditions. In the regions with cold and rainy weather, construction of asphaltic concrete core rockfill dam (ACRD) is easier and more economical than earth core dams. Monitoring of these dams has indicated their good performance during construction and operation for many years [1-2]. However, most of the dams have been constructed in regions with low or moderate earthquake hazard and there is not any publication on actual dam behaviour under severe earthquakes; therefore, the behaviour of asphaltic concrete as an impervious water barrier in high seismic hazard areas needs more attention and exploration [3]. In this study, the data from Shur dam with a height of 85 m (Highest ACRD dam in Iran) was selected as a case study. The response of this kind of core under static and dynamic loading derived from numerical analyses is also presented herein.

2. Previous Numerical and Experimental Studies

Valstad et al. [4] analysed the Storvatn dam located in Norway using Newmark approach. Their

studies indicate that under sever shaking, shearing off of the thin core near the crest may occur. Hoeg [1, 3] presented the results of Storvatn dam and showed that relatively large shear strains may occur in the top of the core if dam slopes are very steep. However, he concluded that rockfill dams with asphaltic concrete core in general have a favourable seismic protection.

Meintjes and Jones [5] analysed the Ceres rockfill dam with asphaltic concrete core located in South Africa using Newmark method and predicted a satisfactory behaviour for the dam. Gurdil [6] performed seismic analysis for the Kopru dam located in Turkey based on the equivalent linear method and concluded that some cracking may occur in the core, near the crest level. However, the self-healing behaviour of asphaltic concrete will solve this problem.

Ghanooni and Mahin-roosta [7] performed dynamic analyses on a typical 115 m height asphaltic concrete core rockfill dam. They concluded that, in nonlinear analysis, the top section of the core experiences small tensile stresses, which are less than asphalt material strength.

Baziar et al. [8] performed some numerical and experimental tests for Meyjaran dam in Iran with a height of 60 m. They concluded that the asphalt concrete core behaves safely under low level of earthquake, but in the moderate and severe earthquake levels, cracking of the asphaltic core in the upper part can develop. Besides, they conclude that the shear modulus of the asphaltic core has no significant influence on the dynamic response of the dam. In another publication, they also approved their numerical analysis with a centrifuge model [9].

Feizi-Khankandi et al. [10] performed a 2D nonlinear analysis on a 125 m typical asphaltic concrete core rockfill dam. They mentioned that the results show the appropriate response of the dam during and after an earthquake shock. Their results show that even under severe earthquake with the maximum acceleration of 0.54 g, the shear strains in the core remains below 0.5%. Mahinroosta and Ravasani [11] after analysing a 110 m typical dam mentioned that the horizontal displacements can be more than 1.5 m in the dam core crest. Wang et al. [12] published a paper on the design and performance of the Yele asphalt-core rockfill dam with the maximum height of 124.5 m. Due to the very high seismicity of the region with an assumed peak horizontal ground acceleration of 0.45 g, the dam is designed with gentle slopes of 1V:2H upstream and 1V:2.2H downstream and a wide crest (14 m). In addition, as an earthquake-resistant measure, geo-grids were placed horizontally to reinforce the top 30 m of the dam.

The first experimental research in the field of seismic behaviour of asphaltic concrete used in hydraulic structures was performed by Breth and Schwab [13]. They concluded that asphaltic concrete behaves as an elastic body under seismic loading. Ohne et al. [14] performed uniaxial cyclic tests on specimens drilled out from Higashifuji dam. They defined and measured the dynamic yield strain for the asphaltic material and concluded that applied compressive stresses can lead to cracking in specimens. Wang [15] reported a series of triaxial cyclic tests on specimens and showed that there was no sign of cracking or degradation on the specimens under the testing conditions used. Nakamura et al. [16] performed some tests to study tensile strength and tensile cracking strain of the asphaltic concrete. The main goal of their study was to investigate the difference between engineering properties of conventional asphaltic concrete with a special admixture (called Super flex-asphalt). They showed that the new type of mix has a higher tensile cracking strain than commonly used asphaltic concrete. Baziar et al. [9] performed a small scale centrifuge modelling of the dam under impact load. They indicated that the numerical results agreed well with the data recorded during centrifuge tests, and the asphaltic core showed similar behaviour in the numerical and centrifuge models. The results of the numerical study for the case study showed that in a severe earthquake, the asphaltic core behaves in a safe manner. Feizi-Khankandi et al. [17] performed an extensive series of monotonic and cyclic tests on triaxial specimens with constant bitumen content at the Norwegian Geotechnical Institute. Temperature and frequency effects on specimen behaviour and specimen degradation were studied under the cyclic loads in both isotropic and anisotropic conditions. Their findings showed that the dynamic shear modulus (G) derived from hysteresis loops were between 1.6 to 4.0 GPa at 5°C and 0.75 to 1.75 GPa at 18°C. They also reported extension behaviour during cyclic loading for some of the specimens at

higher temperature (18°C). Recently, Wang and Hoeg [18] studied the effects of cyclic loading on the stress-strain behaviour and permeability of asphaltic concrete at different temperatures under static and cyclic stress conditions. Their study indicates that at a mean sustained stress of 1.0 MPa, the cyclic modulus (E_d not G) is about 900 MPa at 20°C, 1900 MPa at 9°C, and about 2500 MPa at 3.5°C. They also concluded that the number of loading cycles has no significant effect on the post-cyclic monotonic stress-strain behaviour and permeability (water tightness) of the asphalt concrete.

3. Experimental Work on Asphalt Concrete

Numerous experimental studies carried out showed that dynamic properties of asphaltic concrete is dependent on many factors including initial stress ratio, confining stress, type and frequency of loading, temperature and bitumen content [18-19]. Most of the researches reported in this field relate to the usage of asphaltic concrete as a pavement material and little has been reported on its seismic behaviour especially in warm climate regions because most asphaltic concrete core dams have been constructed in cold regions. Besides, dynamic shear modulus of AC that is needed for nonlinear dynamic numerical analysis has not clearly been addressed in the literature. To obtain the material parameters, an extensive series of monotonic and cyclic triaxial tests were performed and reported by the authors [20].

3.1. Mix Design and Specimen Preparation

Crushed silicate gravel and sand satisfying Fuller distribution given by Eq. (1) was used to manufacture the samples.

$$P_i = 100\left(\frac{d_i}{d_{\max}}\right)^{0.41} \% \quad (1)$$

where P_i is the percentage weight of the material passing sieve size d_i and $d_{\max}$ is the nominal size of the aggregates. B60 type bitumen was used for all tests.

For the AC used as a water barrier, bitumen content between 5.5% and 7.0% is permissible, but researchers commonly advise 6.5 to 7.0 per cent by weight of aggregates [1]. This range of the bitumen content is selected for most of the AC core dams constructed worldwide to achieve flexibility during and after an earthquake loading. Laboratory triaxial specimens were prepared with a mold 100 mm diameter and 200 mm height. The specimens were poured and compacted in four equal thicknesses using the compaction method that results in samples similar to those obtained in field with roller compactors [21].

3.2. Monotonic Triaxial Tests

Monotonic behaviour of AC was investigated using twelve triaxial compression tests. Membrane was used for all the test specimens. All specimens were placed into a constant temperature bath to reach 22°C prior to monotonic testing. The triaxial cell was also filled with de-aerated water at 22°C. All monotonic tests were strain-controlled under compressive loading. After applying the predefined confining stress and reaching a constant temperature, an axial load producing a 2% strain rate per hour was applied until failure. The results of the monotonic triaxial tests are illustrated in Table (1).

Secant modulus in 1% strain was derived from the initial stage of the curves as presented in Table

Table 1. Results of monotonic triaxial tests.

Test Id.	Bitumen Content (%)	σ_3 (kPa)	$E_{1\%}$ (MPa)	σ_1- σ_3 (kPa) at Failure	Axial Strain (%) at Failure	Temperature (°C)
T5.5-1	5.5	250	81	2100	5.3	22
T5.5-2		500	93	3040	6	
T5.5-3		750	151	4090	9	
T6.0-1	6.0	250	53	1842	6.0	22
T6.0-2		500	109	2800	7.8	
T6.0-3		750	118	4000	10	
T6.5-1	6.5	250	46	2050	7.0	22
T6.5-2		500	107	2885	8.2	
T6.5-3		750	76	3725	13.5	
T7.0-1	7.0	250	40	1926	8	22
T7.0-2		500	28	2900	14	
T7.0-3		750	35	3598	16	

(1). For asphaltic concrete material, it is common to use an equation such as Eq. (2) to derive the secant modulus [19]:

$$E_1\% = A \times \sigma_0^y \quad (2)$$

where A and y are constant parameters, and σ_0 is the confining pressure. The value of y is calculated based on the monotonic results reported in Table (1). An example calculation for 7% bitumen content is shown below:

$$E_1\% = A \times \sigma_0^{-0.18} \text{ (Bitumen content} = 7.0\%) \quad (3)$$

3.3. Cyclic Loading Triaxial Tests

Results of 53 cyclic triaxial tests carried out to investigate dynamic properties of asphaltic concrete are reported earlier by authors [19]. The specimens were tested with varying percentages of bitumen content from 5.5 to 7.0% by 0.5% increments and loaded under initial isotropic ($K_c = \sigma_1 / \sigma_3 = 1.0$) and anisotropic initial stress conditions ($K_c = 2.0$ and 3.0). Previous numerical studies indicated that in an actual dam, under an earthquake loading, the top of the dam is affected by a confining pressure of 100 to 500 kPa, so this range of confining pressures was selected in this research. Two types of cyclic loading were applied to the specimens in triaxial tests, type A and type B. In type A, both tension and compression was applied, but in type B, the load was only compressive. In this type of loading, the deviatoric loading reaches a negative value corresponding to axial stress of nearly 0.0 kPa. The majority of tests were carried out using 2 Hz frequency and continued to 50 cycles of Sine wave loading, because most of the energy in a real earthquake is transmitted with 1 to 4 frequency components [22]. An example of the hysteresis loop of the cyclic loading is shown in Figure (1). The hysteresis loops were plotted for the first, tenth and fiftieth cycle of loading for the tests. All specimens showed a compressive behaviour during cyclic loading that means with an increase in number of cycles, residual axial strains develops. Axial stiffness and damping parameters can be derived from the plot of shear stress vs. axial strain. All shear modulus parameters for different cycles were obtained from the upper part (*Gc*) and lower part (*Ge*) of the hysteresis loops because of the difference between the curve inclinations in compression and tension regions. Besides, damping

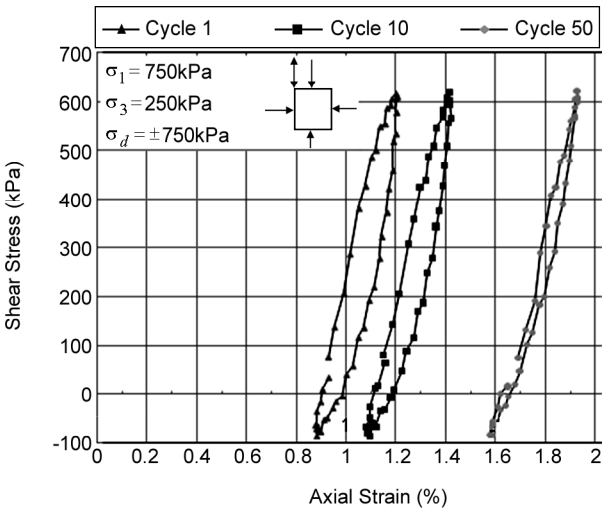

Figure 1. Cyclic stress-strain hysteresis loop, K=3, T=22° σ_3 = 250kPa, Loading type B.

ratio (*D*) was calculated that varied from 0.08 to 0.3. In this temperature (22°C), depending on the bitumen content, confining stress, stress ratio (K_c) and loading type, the shear modulus of the asphaltic concrete varied between 150 to 450 MPa in the compression region (*Gc*) and 80 to 290 MPa in the tension region (*Ge*). An exemplary effect of bitumen content on dynamic shear modulus of the AC is presented in Figure (2). Generally, in higher confining stresses, the higher shear modulus relates to 6.0% and then 5.5% bitumen content. Shear modulus decreases with an increase in bitumen content. However, in low confining stress (100 kPa), the material behaviour is different and a reduction in shear modulus with increasing bitumen content is observed. Therefore, in the upper part of a real dam where the confining pressure is low, using an asphalt mixture with higher bitumen content causes an increase in dynamic shear modulus at strain levels of less than 0.4%. As illustrated in Figure (3), results also indicate that by increasing the confining pressure from 100 to 500 kPa, the average shear modulus increases from 150 MPa to 320 MPa, respectively. By increasing the confining stress, a higher damping value can be seen. An increase in strain-dependent shear modulus, due to an increase in confining pressure, can also be seen from the results.

Increasing the values of K_c caused an increase in the dynamic shear modulus both in tension and compression. This is due to the fact that at higher values of anisotropy state, the amount of the mean

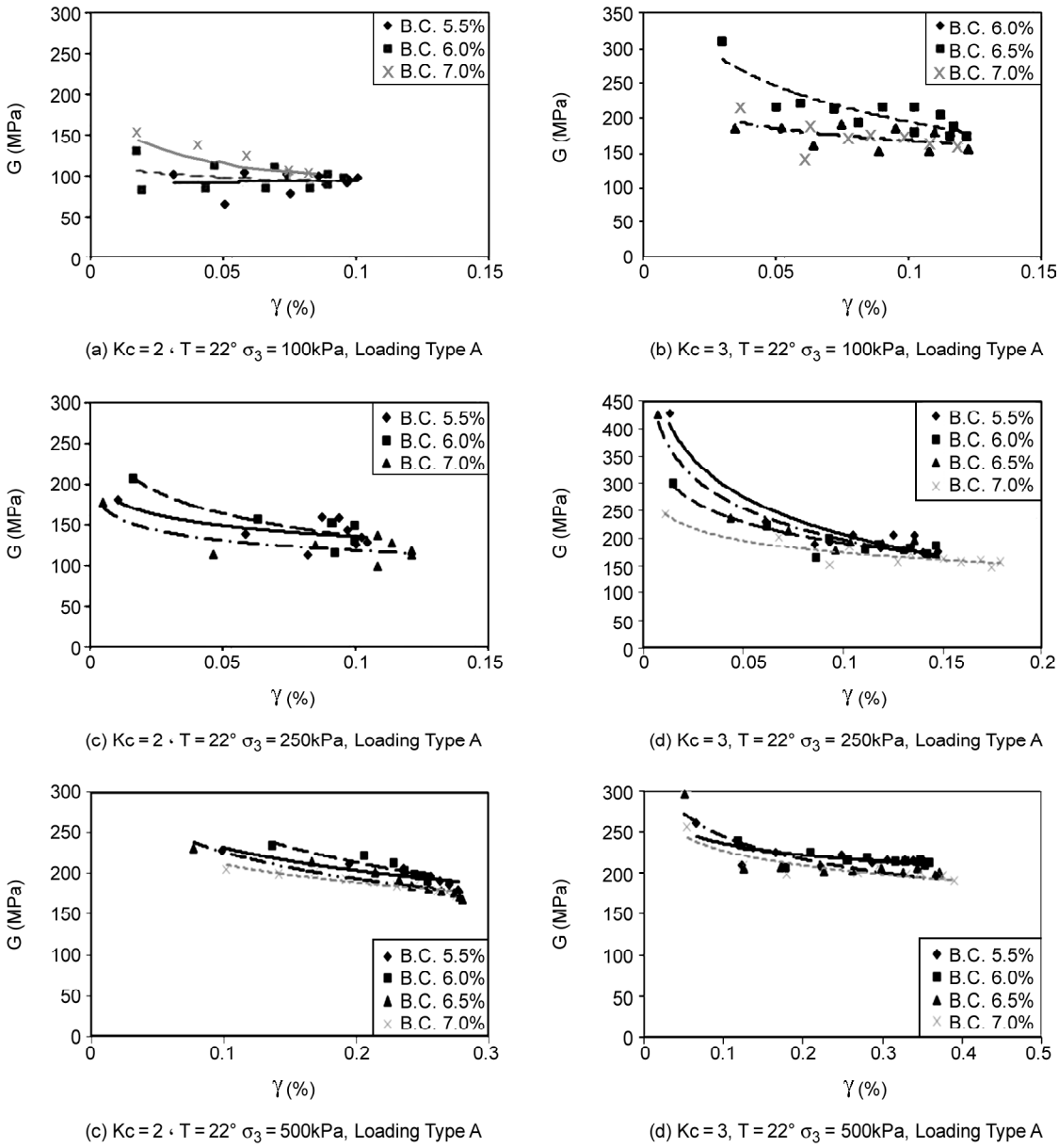

(a) Kc = 2 ، T = 22° σ_3 = 100kPa, Loading Type A

(b) Kc = 3, T = 22° σ_3 = 100kPa, Loading Type A

(c) Kc = 2 ، T = 22° σ_3 = 250kPa, Loading Type A

(d) Kc = 3, T = 22° σ_3 = 250kPa, Loading Type A

(c) Kc = 2 ، T = 22° σ_3 = 500kPa, Loading Type A

(d) Kc = 3, T = 22° σ_3 = 500kPa, Loading Type A

Figure 2. Effect of bitumen content on the strain-dependent dynamic shear modulus.

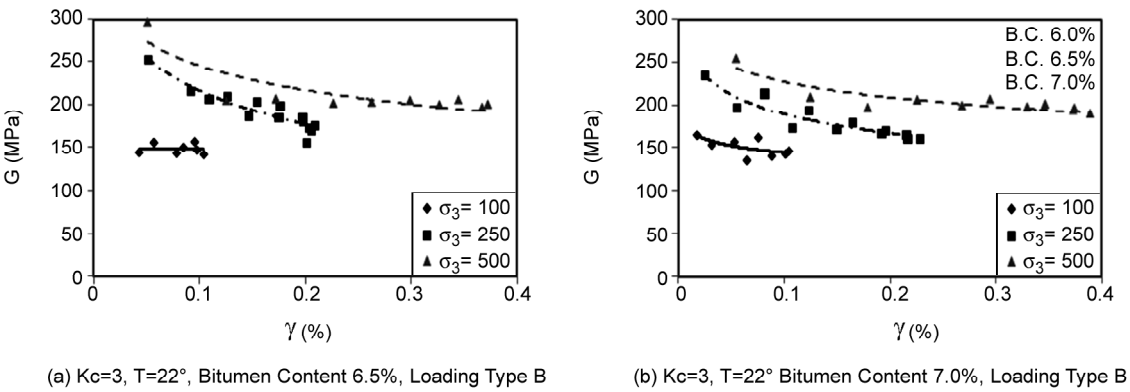

(a) Kc=3, T=22°, Bitumen Content 6.5%, Loading Type B

(b) Kc=3, T=22° Bitumen Content 7.0%, Loading Type B

Figure 3. Effect of confining pressure (kPa) on the strain-dependent shear modulus.

effective stress (σ_{mean}) increases. At a constant confining stress, an increase in the value of K_c results in a decrease in the damping value.

The values of shear modulus are plotted for the 1st, 10th and 50th cycles in Figure (4), it can be observed that by increasing the number of cycles, the amount of shear modulus decreases, but this reduction is not noticeable especially in higher strains.

Assuming a constant poison's ratio during the loading cycle, dynamic shear modulus can be derived from Eq. (4):

$$G = K \times \sigma_0^m \quad (4)$$

where *K* is constant depending on the strain level.

A statistical analysis was performed on the data from all tests with different bitumen content at the same strains and with similar loading conditions, and an average value for power "*m*" at different bitumen content was calculated. For 7% bitumen content, the value derived for m (0.37) is in good agreement with Wang and Hoeg's [18] findings for the asphaltic concrete (0.33) tested at 20°C. Temperature has a significant influence on the results since dynamic shear modulus decreases with an increase in temperature. Their findings also showed that a decrease in temperature from 20°C to 3.5°C can cause a three fold increase in the dynamic modulus. To determine the maximum dynamic shear modulus of the asphaltic concrete, Eq. (4) can be written as:

$$G_{\max} = K_{\max} \times \left(\frac{\sigma_0}{100}\right)^{0.37} \text{ (Bitumen content = 7\%)} \quad (5)$$

where $G_{\max}$ is the maximum shear modulus in MPa and σ_0 is the confining stress in kPa. It can be said that the triaxial test does not have sufficient accuracy in a small strain range, so Gmax cannot be calculated directly from test data. Extrapolation from the shear modulus-shear strain curve has to be used to obtain the small strain shear modulus ($G_{\max}$). Nakamura et al [16] suggested a $G/G_{\max}$ vs. γ curve for the asphalt concrete used as an impervious core in embankment dams. Results of the middle range of strains obtained in triaxial tests show good compatibility in comparison with the adopted G-γ curve from Nakamura et al. [16]. A statistical analysis was performed on all the triaxial test results for 7% bitumen content in different levels of strains and $K_{\max}$ was determined as follows:

$$G_{\max} = K_{\max} \times \left(\frac{\sigma_0}{100}\right)^{0.37}, K_{\max} = 321 \quad (6)$$

where: $100 < \sigma_0 < 500$ (kPa)

Eq. (6) can be used for nonlinear numerical dynamic analyses in conjunction with Nakamura's suggested curve for $G/G_{\max}$.

4. Finite Difference Analysis

4.1. Overview

2D and 3D dynamic deformation analysis of the Shur river dam was performed using FLAC program and its built-in elasto-plastic model of Mohr-Coulomb [23-24]. In order to model variations in properties of the embankment materials with effective stress, (i.e. friction angle and shear modulus in dynamic analysis) a number of functions were developed using software's built-in programming language, FISH. Moreover, FISH has been used to introduce hyperbolic nonlinear model in static analysis.

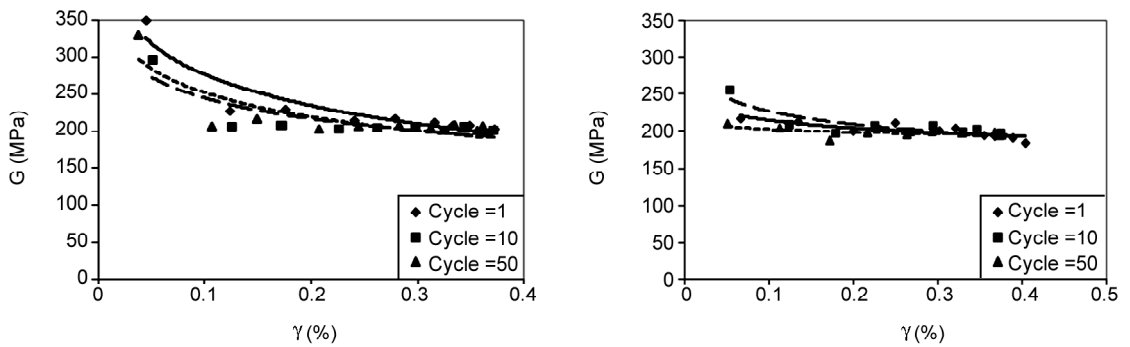

Figure 4. Effect of number of cycles on the strain-dependent shear modulus.

4.2. The Shur River Dam

Shur dam that is under construction in south of Kerman province, is the highest asphalt concrete core rockfill dam in Iran. It has a height of about 85 meters and is located in a U-shaped long valley. The crest length of the dam is about 450 m and the vertical asphaltic concrete core, as a watertight element, has 1.2 m width at the bottom decreasing to 0.6 m on the top, and is surrounded by filters (zones 2a) and transitions in upstream and downstream (zones 2b). The seismicity of the region is very high with MDE equal to 0.8 g [25]. Figure (5) illustrates the location and cross section of the dam.

The simplified embankment model and the finite difference mesh used in 2 and 3 dimensional analysis are shown in Figure (6). Based upon the elastic properties of the dam materials, the compression and shear wave speeds are taken as [25]: C_p = 753 m/sec, C_s = 413 m/sec

For accurate representation of wave transmission in the model during dynamic analyses, the spatial element sizes were selected small enough to satisfy the following criteria expressed by Kuhlemeyer and Lysmer [26]:

$$Dl \le \frac{\lambda}{10} \tag{7}$$

where λ is the wave length associated with the highest frequency component that contains appreciable energy and l is the length of the element.

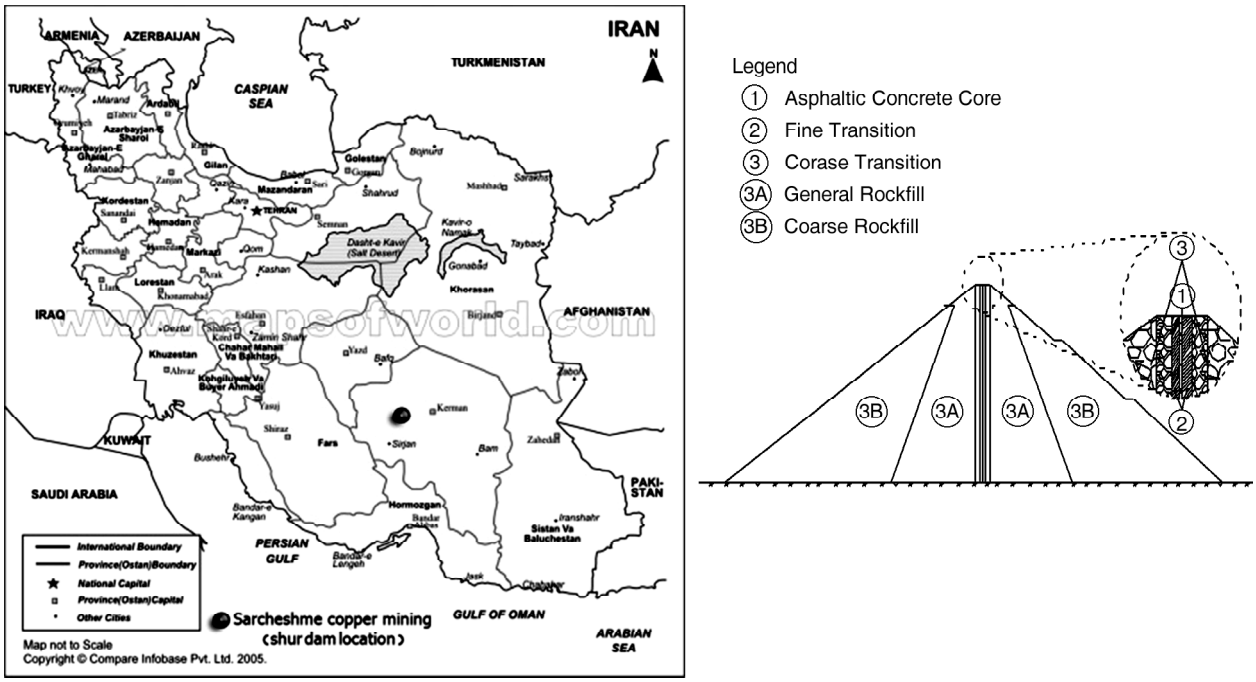

Figure 5. Location and typical cross section of the Shur dam.

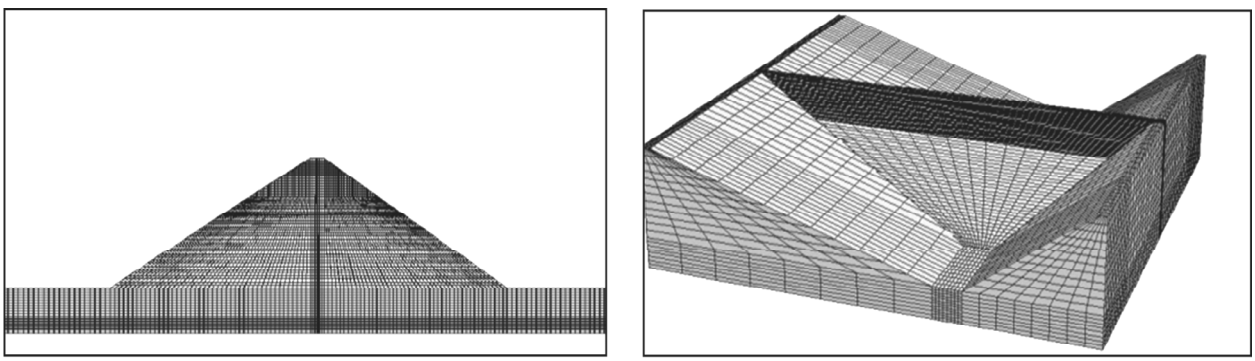

Figure 6. 2 and 3D Finite Difference Grid Generation.

4.3. Static Analysis

Static analyses were carried out for various stages including the end of construction and impounding. The hyperbolic model proposed by Duncan and Chang [27], was used in these analyses. Tables (2) and (3) present the material properties used for numerical analyses.

The end of construction analyses were performed using staged construction in 45 layers. Figures (7) and (8) show the vertical and horizontal displacement contours in the highest section of dam for 3D analysis. The maximum settlement occurs inside the shell.

The amount of maximum settlement is nearly 390 mm. Horizontal displacement has symmetric contours with the maximum of 190 mm. These values for 2Danalyses are 440mm and 200mm respectively. Results show that third dimension has no significant effect on the static displacements, which is due to the long valley of the dam site.

The impounding stage was performed by increasing water level to a height of 80 m above the base at three stages. During impounding, the hydrostatic force acts on the surface of the asphalt core because permeability of asphalt concrete in comparison with the shell and transition materials is very low. The adopted mobility coefficients and porosities for different materials are presented in Table (4). A coupled flow and mechanical analysis was performed for modelling this stage. Figure (9) shows the predicted pore pressure contours after first filling to full supply level. The pattern of the pore pressure contours appears to be reasonable.

Table 2. Mohr-coulomb properties for asphaltic concrete.

Material	γ (Kg/m^3)	E (MPa)	υ	C (kN/m^2)	φ	ψ
Asphalt	2420	40	0.49	360	18	0

4.4. Dynamic Analysis

ATC Consulting Engineers Co. [25] in their seismicity report for the dam site has proposed three alternative ground motion records suitable for

Table 3. Hyperbolic properties for rockfill and transitions.

Material	γ (Kg/m^3)	k_i	K_b	K_{ur}	n	m	R_f	C (Pa)	φ	$\Delta\varphi$
Rockfill	2200	400	250	700	0.65	0.5	0.7	0	46	3
Transition	2150	200	150	400	0.4	0.5	0.7	0	38	4

Table 4. Embankment material hydraulic properties.

Material	Bedrock	Asphalt Core	Zones 2a/2b	Zone 3
Mobility Coefficient (m^2/Pa.s)	$1x10^{-10}$	$1x10^{-15}$	$1x10^{-8}$	$1x10^{-6}$
Permeability (m/s)	$1x10^{-6}$	$1x10^{-11}$	$1x10^{-4}$	$1x10^{-2}$

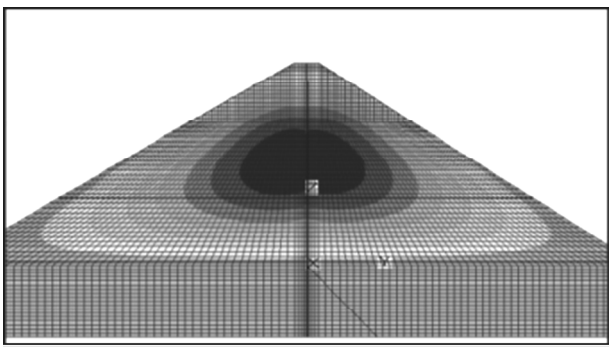

Figure 7. Vertical displacements contours at the end of construction stage (3D analysis).

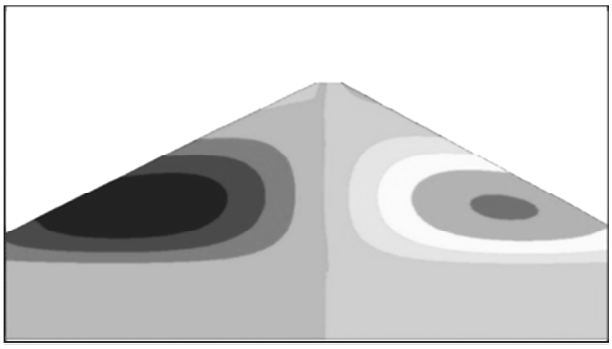

Figure 8. Horizontal displacements contours at the end of construction stage (3D analysis).

seismic analysis. From the two horizontal components of the acceleration-time histories the most severe component was used for the modelling. All waves were normalized to MDE acceleration. Figure (10) shows time histories of the earthquakes used in the analysis.

Most of the energy in the input motions is at frequencies less than 15, 15 and 20 Hz for Loma Prieta, Cape Mendocino and Nahanni earthquakes respectively. The seismic records were filtered to remove frequencies greater than the above frequencies. The filtering process was performed to limit the size of elements and to ensure accurate wave transmission. After filtering was completed, the waves were corrected for a base line drift (i.e. continuing residual displacement after the motion has finished). Finally, the input motion to the model was applied as a shear stress boundary in order to

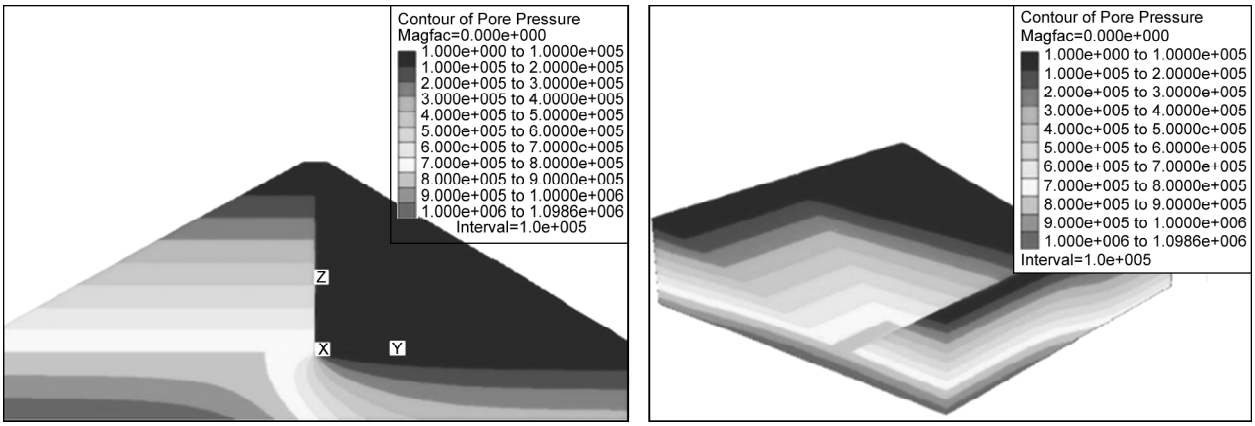

Figure 9. Pore pressure contours after impounding.

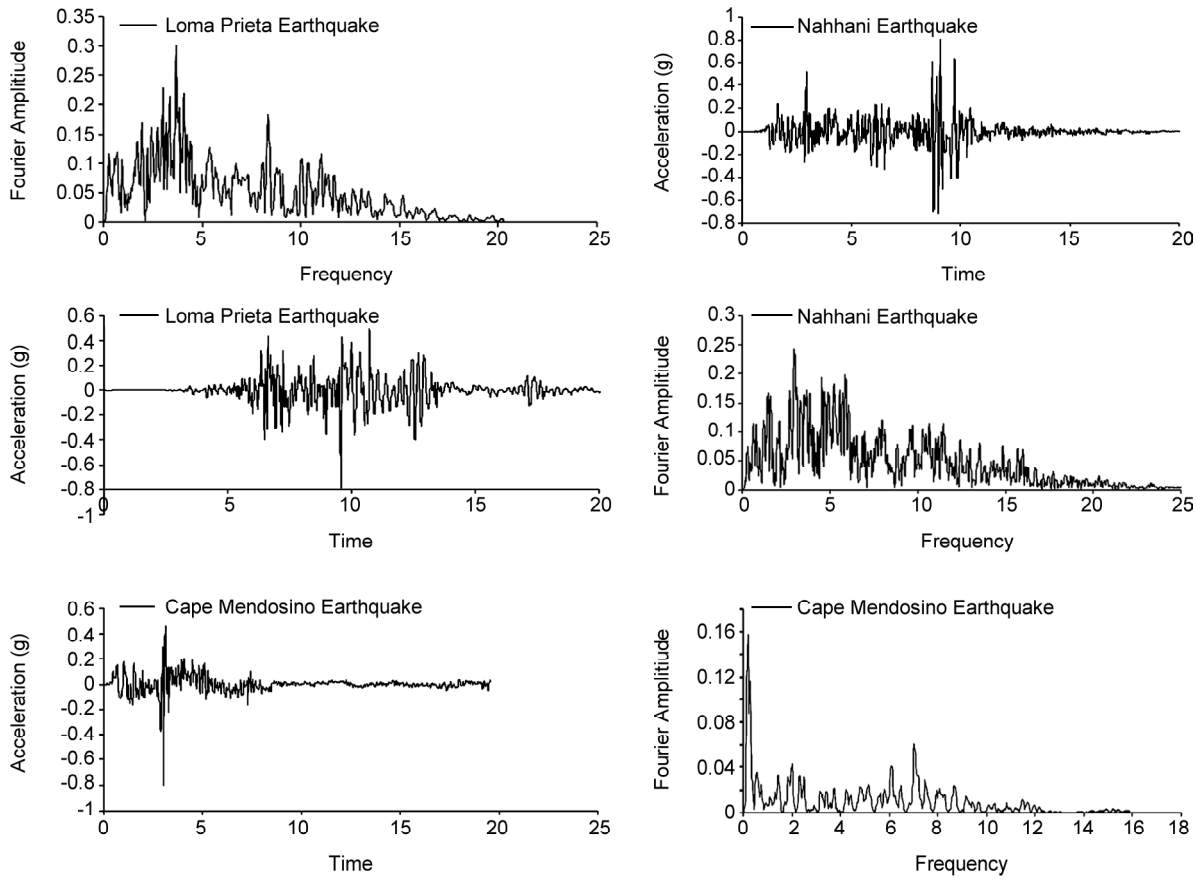

Figure 10. Time history and frequency domain for Nahanni, Loma Prieta and Cape Mendocino earthquakes.

establish quiet boundary conditions along the same boundary as the dynamic input, as suggested by the software manual.

4.4.1. Material Properties

Stiffness and damping properties of the embankment materials used in the FDM analysis are summarized in Table (5), and are discussed underneath.

Table 5. Dynamic properties of embankment material.

Material	Poisson's Ratio	Shear Modulus G (MPa)	Modulus Reduction & Damping Curve
Bedrock	0.23	2,700	Schnabel (1973)
Asphalt	0.49	$321(\sigma_m/100)^{0.37}$	Nakamura (2004)
Zone 2	0.3	$*19.8\ \sigma_m^{0.5}$	Ishibashi (1993)
Zone 3	0.23	$*37.4\ \sigma_m^{0.5}$	Ishibashi (1993)

$*\sigma_m$ is the mean effective stress

Douglas [28] after analysing a large database of test results developed Eq. (8) for shear strength of rockfills [29]:

$$\sigma_1' = RFI.\sigma_3'^{\alpha} \tag{8}$$

where σ_1 and σ_3 are major and minor principal stress. The best estimation for α is 0.8726 and RFI is a multiplier depending on initial porosity, angularity, maximum particle size, percent of fines and unconfined compressive strength. RFI is taken as 4.8607 for the Shur dam rockfill [20]. The lower and upper bound shear strength from all data and adopted profile for Shur dam rockfills is illustrated in Figure (11).

The small strain shear modulus, Gmax, was determined using the methods described by Kramer [22] and the seismic refraction test results of the main dam foundation area [25]. In the early stages of dynamic analysis using the relevant FISH corresponding to the confining stress (which was assumed equal to the average stress), dynamic shear modulus for all elements of the dam is calculated; therefore, each element of the grid has its own specific modulus. Gmax for the bedrock was calculated using the average shear wave velocity of 1050 m/s (measured in seismic refraction tests). For zones 2 and 3, the Gmax values were determined using the empirical

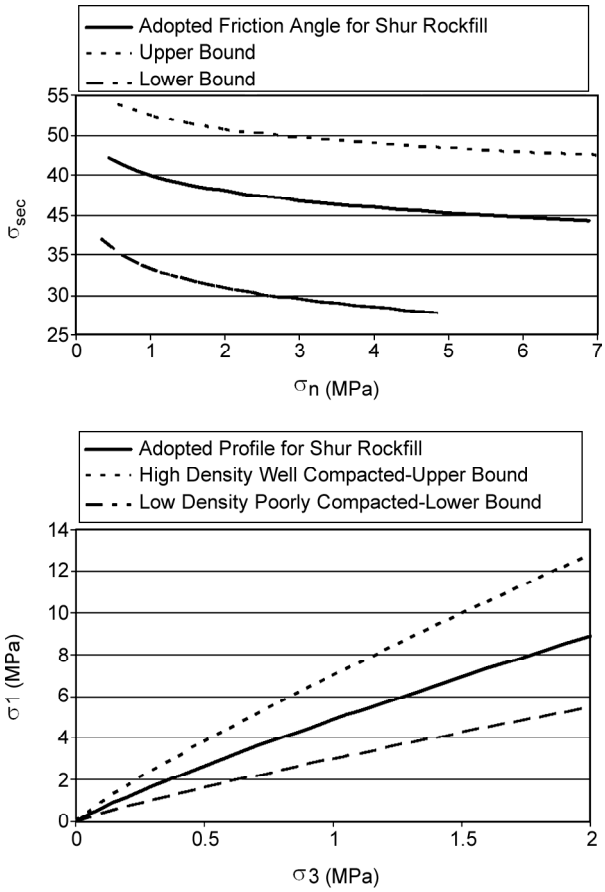

Figure 11. Maximum principal stress vs. minimum principal stress (σ1 vs. σ3) and secant friction angle of rockfill vs normal stress (σsec vs. σn) (RFI=4.8607).

relationship developed by Seed and Idriss [30] as follows:

$$G_{\max} = 220K_{2\max}.\sigma_m^{0.5} \tag{9}$$

where $K_{2\max}$ is the shear modulus coefficient and it is a function of relative density and soil types. For a good quality rockfill (i.e. Zone 3), $K_{2\max}$ ranges from 120 at the surface to 180 at a depth of 100m. A value of 170 was adopted for Zone 3 rockfill. For the transition zones (Zone 2) a value of 90 was adopted [29]. Based on the large number of triaxial tests on the asphaltic concrete performed by Akhtarpour and Khodaii [19], an equation was developed for $G_{\max}$ of the asphalt in 22°C temperature as below:

$$G_{\max} = K_{\max}.\left(\frac{\sigma_m}{100}\right)^{0.37}, K_{\max} = 321 \tag{10}$$

An initial damping ratio of 1% was assumed for all materials as the hysteretic damping shown in Figure (12) could not completely damp the high

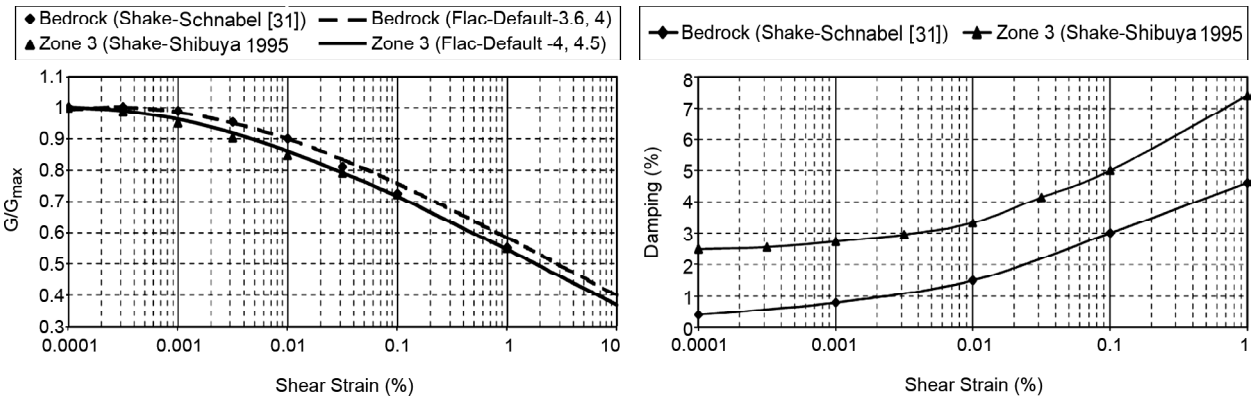

Figure 12. Variation in shear modulus and damping curves for zones 2 and 3 and bedrock.

frequency components of the dynamic inputs. The variation of shear modulus with strain level for each of the zones of the dam body was automatically updated during the analysis using hysteretic type damping. The adopted curves for bedrock are from Schnabel [31], and the curves for Zone 2 and Zone 3 are from Ishibashi and Zhang [32]. These curves were used to derive the material properties needed in the numerical model via the built-in default hysteretic model. The default hysteretic is the curve shaped model of modulus versus logarithm of cyclic strain, which has been represented by a third degree equation, with zero slopes at both small and large strain. This model requires two parameters, $L1$ and $L2$ that were obtained by curve fitting on the modulus reduction curves.

The Adopted Curves for Asphaltic Concrete are from Nakamura et al. [16] using curve fitting method on default build-in hysteretic model. Figure (13) illustrates assumed curves for asphaltic core. As it can be seen, the built-in default hysteretic model has some deviation from Nakamura, especially in middle range of shear strains.

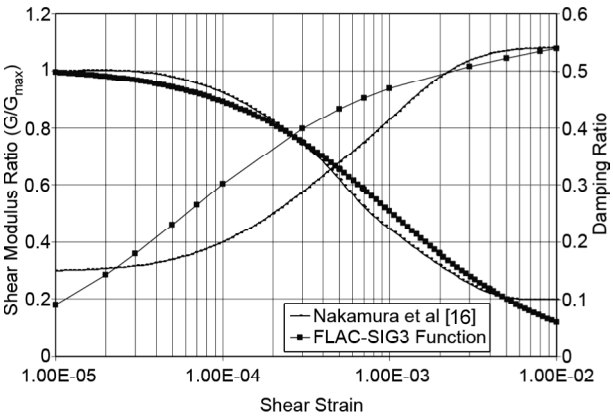

Figure 13. Reduction of shear modulus and damping ratio for asphaltic concrete core.

5. Analysis of Results

The general pattern of deformation as a result of seismic loading is shown in Figure (14). It is evident that the predicted pattern of deformation involves settlement and slumping of the rockfill on either side of the core, while in 2D analyses the core generally remains upright, protruding from the slumped rockfill, with some lateral deformation. This is in agreement with typical behaviour reported of this type of dams [8-10].

However, in the case of 3D analysis, the asphaltic core settles with the downstream shell. The main reason is possibility of lateral displacements in the asphaltic core that can lead to settlement of the core. As an example, Crest acceleration and vertical deformation as a function of time are shown in

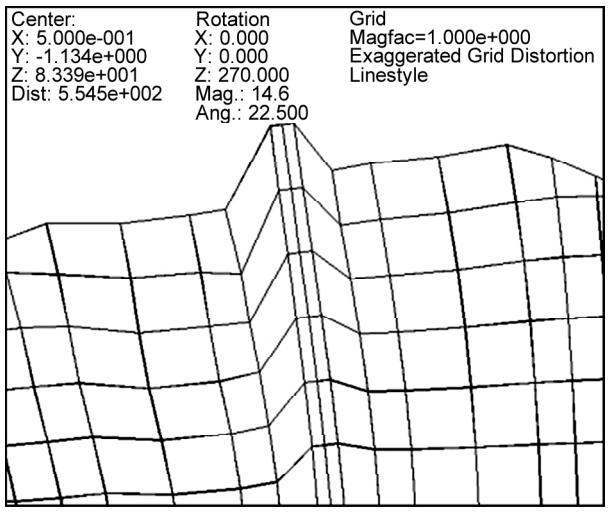

Figure 14. General pattern of deformation (2D analysis).

Figures (15) and (16), for the Loma Prieta ground motion record in 2D and 3D analysis respectively. The results of the analyses are summarized in Table (6).

The predicted peak crest acceleration for 2D analysis varies between 0.99 g to 1.2 g as compared to the input peak acceleration of 0.8 g implying an amplification of 1.24 to 1.5. For the 3D analysis, these values are 1.1 g to 1.37 g for crest acceleration and 1.37 to 1.71 for amplification factor. These

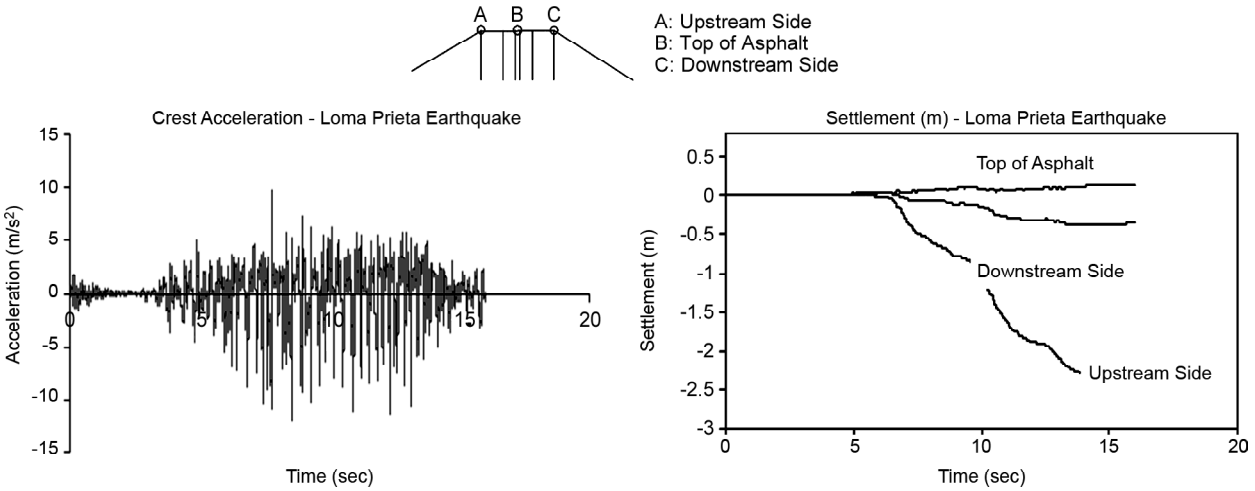

Figure 15. Crest acceleration and vertical deformation vs. time for Loma Prieta earthquake (2D analysis).

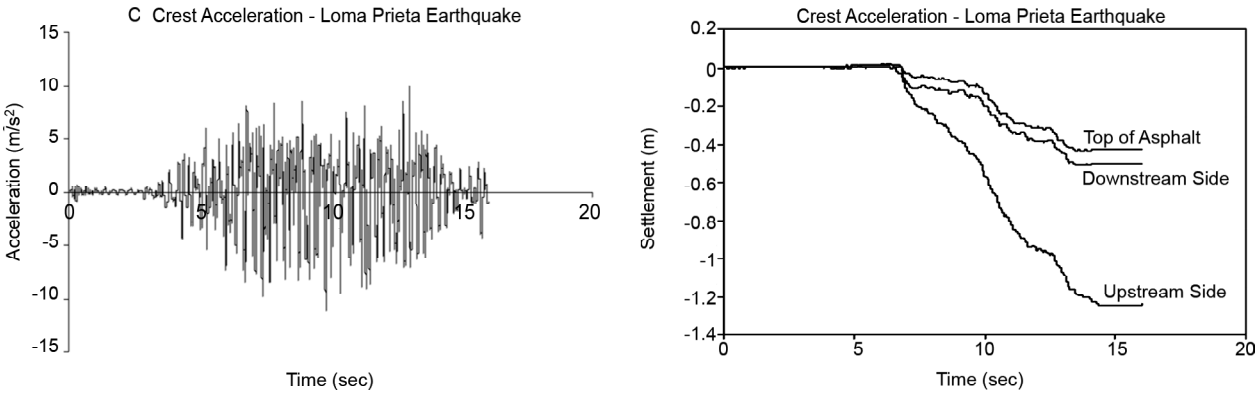

Figure 16. Crest acceleration and vertical deformation vs. time for Loma Prieta earthquake (3D analysis).

Table 6. Summary of Predicted Displacements (2D and 3D).

Earthquake (2D Analysis)	Peak Crest Acceleration (g)	Predicted Crest Settlement (m)			Core Horizontal Relative Displacement (m)
		U/S	Core	D/S	
Loma Prieta	1.189	-2.34	0.13	-0.36	-1.702
Cape Mendocino	0.99	-1.13	0.18	-0.04	-0.607
Nahanni	1.202	-1.88	0.22	-0.17	-1.341
Earthquake (3D Analysis)	**Peak Crest Acceleration (g)**	**Predicted Crest Settlement (m)**			**Core Horizontal Relative Displacement (m)**
		U/S	Core	D/S	
Loma Prieta	1.114	-1.207	-0.41	-0.45	-1.22
Cape Mendocino	1.143	-0.62	0.01	-0.02	-0.30
Nahanni	1.378	-1.016	-0.1	-0.12	-0.72

[1] Positive horizontal displacements indicates movement in the downstream direction and vice versa

ranges of amplifications are expected for rockfill embankment dams based on past experience reported in many studies. It is evident that the predicted highest vertical displacement occurs at the embankment crest. These displacements attenuate rapidly with depth and indicate no evidence of significant movements of concern. The maximum crest vertical settlement resulted from the Loma Prieta ground motion record was 2.34 m, Figure (15), in the case of 2D analysis and 1.21 m, Figure (16), for 3D analysis. The results of the FDM analysis indicate that the maximum deformations will occur near the crest and at the lower part of the upstream slope. The magnitude of the estimated deformations appears to be large but would not be sufficient to cause loss of storage under normal operating conditions. Shear strains and lateral displacement in centre of the embankment core resulting from each of the ground motion records analysed, are shown in Figure (17). It can be seen that the predicted maximum relative lateral deformation of the core is approximately 1.70 m at the embankment crest in the case of 2D analysis and 1.22 m in the case of 3D analysis, resulting from the Loma Prieta ground motion record. While the predicted maximum horizontal deformation of 1.70 m does exceed the 0.6 m width of the asphalt core, this deformation is associated with slumping in the upstream face of the embankment, thus one can suggest that complete disassociation of the thin core is not probable. At the levels of shear

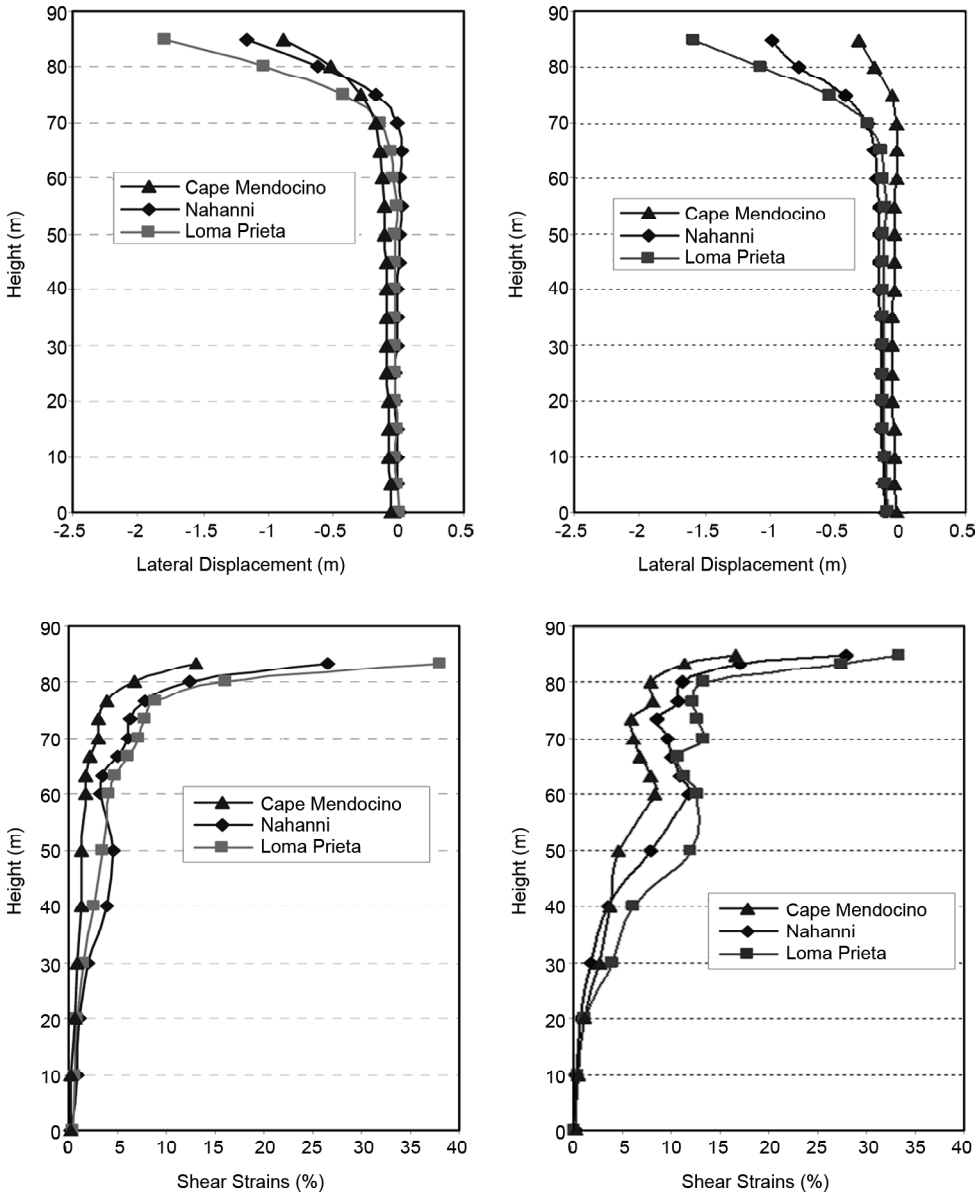

Figure 17. Shear strains and lateral displacement of asphaltic core after earthquake loading (A): 2D analysis (B):3D analysis.

strains observed, plastic deformation of the core is expected, and cracking of the core may occur in the upper 15 meter of the dam. Remaining shear strains in the case of 2D analysis varies between 4~7 % at 15 meter below crest level to about 19% at normal water level. In the case of 3D analysis these values are between 4~10 % at 15 meter below crest level to about 10% at the normal water level. Experimental studies show that it can lead to developing some cracks and increasing permeability of asphaltic core [1]; therefore, concentrated seepage can occur in the upper part of the thin core in the case of very severe earthquakes.

6. Conclusions

- During the dynamic loading, different displacements between the thin core and transition layers are observed especially in case of 2D analysis.
- Peak crest accelerations in the case of 3D analysis are more than 2D peak accelerations, but displacements resulted from 2D analysis are more than that obtained in 3D analysis.
- The pattern of the core deformation in 2D analysis includes settlements of the shells behind the asphaltic core and the core remains upright, but 3D analysis shows that the core can settle with the neighbouring shells.
- The maximum predicted deformation of the rockfill is a vertical deformation of 2.34 m and 1.21 m for 2D and 3D analysis respectively, determined using the finite difference method. Under normal operating conditions, a minimum freeboard of 4.0 m is provided between crest level and spillway level; thus, deformations of this magnitude would not cause the storage to be breached.
- Based on the predicted deformation of the embankment core and estimated level of internal shear strain in the core material, complete disassociation of the embankment core is not to be expected, but developing cracks and increasing permeability in higher part of core may occur.
- It is essential that the downstream transitions and downstream shell and toe should be designed with adequate drainage capacity to handle concentrated leakage and prevent dam failure even if the temporary water loss is dramatic.
- Based on the numerical analysis, lateral displacements above 70 meters height increases rapidly, hence it seems that the reduction in core thickness with the height of the dam, as considered in design, is not appropriate.
- Numerical analysis indicate that in an actual dam subjected to a very severe earthquake, the remaining plastic shear strains might be considerably more than 0.4% in the top third of the asphaltic core, but the lower part experiences less shear strains, it is therefore advisable to use higher bitumen content in the upper part to ensure more flexibility and prevent tensile cracking strain and lower bitumen content in the lower part considering financial advantages.
- The study of dynamic behaviour of AC subjected to cyclic loading, indicate that even under moderate earthquake the AC retains its stability if used as a water barrier in a rockfill dam.
- Suitable bitumen content in the mix depends on the dynamic shear strains, ambient temperature and bitumen type. Results of this study show that in the low level of shear strains (lower part of the asphaltic core), lower bitumen content can be used without significant reduction in flexibility of the asphaltic concrete.

References

1. Hoeg, K. (1993) *Asphaltic Concrete Cores for Embankment Dams*. Norwegian Geotechnical Institute of Technology, Oslo, Norway.

2. ICOLD Press (1984 and 1992) Bituminous cores for earth and rockfill dams. *Bulletin*, 42 and 84.

3. Hoeg, K. (2005) *Earthquake Resistance of Asphaltic Concrete Core*. Annual report from NGI publications.

4. Valstad, T., Selness, P.B., Nadim, F., and Aspen, B. (1991) Seismic response of a rockfill dam with an asphaltic concrete core. *Journal of Water Power and Dam Construction*, **43**, 1-6.

5. Menitijees, H.A. and Jones, C. (1999) Dynamic analyses of the new cores dam. *12th Regional Conference for Africa on Soil Mechanics and Geotechnical Engineering*, Durban, South Africa.

6. Gurdil, A.F. (1999) Seismic behaviour of asphaltic concrete core dams. *Proc. 1st Symposium on*

Dam Foundation, Antalya, Turkey.

7. Ghanooni, S. and MahinRoosta, R. (2002) Seismic analysis and design of asphaltic concrete core dams. *Journal of Hydropower and Dams*, **9**(6), 75-78.

8. Baziar, M.H., Salemi, Sh., and Heidari, T. (2006) Analysis of earthquake response of an asphalt concrete core embankment dam. *International Journal of Civil Engineering*, IUST, **4**(3).

9. Baziar, M.H., Salemi, S.H., and Merrifield, C.M. (2009) Dynamic centrifuge model tests on asphalt-concrete core dams. *Geo Technique*, **LIX**(9).

10. Feizi-Khankandi, S., Ghalandarzade, A., Mirghasemi, A.A., and Hoeg, K. (2009) Seismic analysis of Garmrood dam with asphaltic concrete core. *Soils and Foundation*, **49**(2), 153-66, DOI: 10.3208/sandf.49.153.

11. Mahinroosta, R. and Ravasani, A. (2009) Dynamic response of an asphaltic concrete core embankment dam considering core and filter interaction. *2nd Int. Conf. on Long Term Behaviour of Dams*, Graz, Austria, 654-659.

12. Wang, W., Hoeg, K., and Zhang, Y. (2010) Design and performance of the yele asphalt core rockfill dam. *Canadian Geotechnical Journal*, **47**(12).

13. Breth, H. and Schawab, H. (1973) *ZurEignung Des Asphalt Betons fur die Innendictung Von Staudammen*. Wassewirtschaft Stuttgart, Germany; 69, Heft 11, 348-51. (In German)

14. Ohne, Y., Nakamura, Y., Okumura, T., and Narita, K. (2002) Earthquake damage and its remedial measure for earth dams with asphalt facing. *Proc. 4th Int. Conf. on Dam Engineering*, 18-20, China.

15. Wang, W. (2005) *Cyclic Tests on Asphalt Concrete*. Xi'an University Press, China, (In Chinese).

16. Nakamura, Y., Okumura, T., Narita, K., and Ohne, Y. (2004) Improvement of impervious asphalt mixture for high ductility against earthquake excitation. *Proc. of 4th International Conference on Dam Engineering*, China, 18-20.

17. Feizi-Khankandi, S., Mirghasemi, A, Ghalandarzadeh, A., and Hoeg, K. (2008) Cyclic triaxial tests on asphaltic concrete as water barrier for embankment dams. *Journal of Soils and Foundations, Japanese Geotechnical Society*, **48**(3), 319-332.

18. Wang, W. and Hoeg, K. (2011) Cyclic behaviour of asphalt concrete used as impervious core in embankment dams. *Journal of Geotechnical and Geo Environmental Engineering*, **37**(5), 536-44.

19. Akhtarpour, A. and Khodaii, A. (2013) Experimental study of asphaltic concrete dynamic properties as an impervious core in embankment dams. *Construction and Building Materials*, **41**, 319-334.

20. Akhtarpour, A. (2011) *Numerical and Experimental Evaluation of the Dynamic Behaviour of the Asphaltic Concrete Core Rockfill Dams*. Ph.D. Dissertation, Amirkabir University of Technology, Tehran, Iran.

21. Wang, W. and Hoeg, K. (2002) Effects of compaction method on the properties of asphalt concrete for hydraulic structures. *Internation Journal Hydropower and Dams*, **6**, 63-71.

22. Kramer, S. (1996) *Geotechnical Earthquake Engineering*. Prentice-Hall International Series in Civil Engineering Mechanics (USA), January.

23. Itasca Consulting Group (1998) Fast Lagrangian Analysis of Continua, Minneapolis. Minnesota, USA.

24. Vermeer, P.A. and de Borst, R. (1984) Non-Associated Plasticity for Soils, Concrete and Rock. *Heron*, **29**(3), 1-64, (Quoted by Itasca).

25. Australian Tailing Consultants, ATC (2008) Design Report, Shur River dam.

26. Kuhlemeyer, R.L. and Lysmer, J. (1973) Finite element method accuracy for wave propagation problems. *Journal of Soil Mechanics and Foundations*, Div. ASCE, **99**(SM5), 421-427.

27. Duncan, J.M. and Chang, C.Y. (1970) Nonlinear analysis of stress and strain in soils. *Journal of Soil Mechanics and Foundation Division*,

ASCE, **96**(5), 1629-53.

28. Douglas, K.J. (2002) *The Shear Strength of Rock Masses*. Ph.D. Dissertation. School of Civil and Environmental Engineering, Sydney Australia, Chapter 4.

29. Seed, H.B., Wong, R.T., Idriss, I.M., and Tokimatsu, K. (1984) Moduli and damping factors for dynamic analyses of cohessionless soils. *Journal of Geotechnical Engineering*, **112**(11), 1016-1032.

30. Seed, H.B. and Idriss, I.M. (1970) Soil Moduli and Damping Factors for Dynamic Response Analyses. Report EERC 70-10, Earthquake Engineering Research Centre, University of California, Berkeley.

31. Schnabel, P.B. (1973) *Effects of Local Geology and Distance from Source on Earthquake Ground Motion*. Ph.D. Dissertation, University of California, Berkeley, California.

32. Ishibashi, I. and Zhang, X.J. (1993) Unified dynamic shear module and damping ratios of sand and clay. *Soils and Foundations*, **33**(1), 182-191.